

## **TRACKING OBJECTS OF DEFORMABLE SHAPES**

**K. Mahesh**

Associate Professor, Department of Computer Science and Engg  
Alagappa University, Karaikudi, TN, India.  
mahesh.alagappa@gmail.com

**Dr.K.Kuppusamy**

Associate Professor, Department of Computer Science and Engg  
Alagappa University, Karaikudi, TN, India.  
kkdisamy@yahoo.com

**G. Radha Priyadharsini**

Department of Computer Science and Engineering  
Alagappa University, Karaikudi, TN, India.  
rpgmphil@gmail.com

### **ABSTRACT**

We propose a solution to determine the optimal elastic matching of a deformable template to an image. The central idea is to cast the optimal matching of each template point to a corresponding image pixel as a problem of finding a minimum cost cyclic path in the three-dimensional product space as well as in four-dimensional product space spanned by the template and the input image. We introduce a cost functional associated with each cycle, which consists of three terms: a data fidelity term favoring strong intensity gradients, a shape consistency term favoring similarity of tangent angles of corresponding points, and an elastic penalty for stretching or shrinking. The functional is normalized with respect to the total length to avoid a bias toward shorter curves. Optimization is performed by Lawler's Minimum Ratio Cycle algorithm parallelized on state-of-the-art graphics cards. The algorithm provides the optimal segmentation and point correspondence between template and segmented curve in computation times that are essentially linear in the number of pixels. A new approach to 4-D shape-based segmentation and tracking of multiple, deformable anatomical structures used in cardiac MR images can be implemented here. We propose to use an energy-minimizing geometrically deformable template (GDT) which can deform into similar shapes under the influence of image forces. The degree of deformation of the template from its equilibrium shape is measured by a penalty function associated with mapping between the two shapes. By minimizing this term along with the image energy terms of the classic deformable model, the deformable template is attracted towards objects in the image whose shape is similar to its equilibrium shape. This allows the simultaneous segmentation of multiple deformable objects using intra- as well as inter-shape information. Simulated Annealing (SA), a stochastic relaxation technique is used for segmentation while Iterated Conditional Modes (ICM), a deterministic relaxation technique is used for tracking.

**Keywords:** Image segmentation, tracking, elastic shape priors, discrete optimization, dynamic programming, minimum ratio cycles, Simulated annealing, real-time applications

## 1. INTRODUCTION

IMAGE segmentation and the tracking of objects are two of the most prominent topics in computer vision. Numerous authors have tried to solve these problems based on low level information such as edges or region statistics [25], [34],[3], [42], [21]. However, their success has been limited: In real-world images, the low-level information is often corrupted, e.g., by changing lighting conditions and low contrast between object and background. As an example, consider Figure. 1, where a car is tracked in rainy weather. To cope with such challenges, researchers have endeavored to integrate prior knowledge into the respective segmentation processes. In numerous studies [19], [4], [13], [7], this was shown to significantly improve the resulting segmentations. However, most of these methods find local minima, and hence, require an initialization in the vicinity of the solution. The one that does find globally optimal segmentations [13] has a quadratic memory complexity. It is hence well suited for tracking tasks, but for pixel-accurate image segmentation, only rather coarse resolutions can be handled. In this work, we present the first globally optimal shape based segmentation method able to yield pixel-accurate segmentations in effectively linear time.

The segmentation problem in complex images cannot be addressed adequately without the anatomical a-priori knowledge which usually aids in making decisions about the image segmentation. In this case two major sources of a-priori knowledge can be identified:

A-priori information about the mean shape and the variability of anatomical objects.

A-priori information about the mean location, orientation and size of the objects with respect to each other and their variability.

Here we address the segmentation and tracking problem in these images using Geometrically Deformable Templates (GDT).This novel approach differs in the following points from previously described models: Its deformation is controlled via a penalty function rather than via its parameterization .This penalty function is associated with a thin-plate spline(TPS)mapping function which maps the templates in its equilibrium configuration into a deformed configuration. One can visualize thin plate spline mapping function as an imaginary rectangular grid associated with the model in equilibrium. Any deformation of the model would also deform the rectangular grid. The penalty function requires energy for any non-affine deformation of the grid but does not penalize affine deformations. Moreover , the model can incorporate not only information about the mean location, orientation and size of the anatomical objects with respect to each other and their variability. Thus , the model can be used to segment multiple objects simultaneously.

### 1.1 Related Work

Image segmentation and tracking are closely related problems, yet each with its own history. We, therefore, review them separately.

#### 1.1.1 Tracking Deformable Objects

The tracking of objects has traditionally been based on feature points [17], [22]. Starting from the KLT-tracker [42],subsequent feature-based methods appeared in [21], [30].More recently, methods have become popular that treat the object as an entity [11], [6], [20] rather than an independent number of parts. Denzler and Niemann [11] consider a set of patches that is linked by a ray model. Cremers [6] models the temporal evolution of shapes by a dynamical, autoregressive model in a level set framework. This is extended by Gui et al. [20] to the case of competing priors. While many of these methods are based on minimizing a suitable energy, none guarantees to find the global optimum. However, such methods give neither a guarantee to find good (i.e., low energy) solutions nor a means to verify if a solution is optimal. To determine

global optima in the presence of significantly deforming curves has remained an open challenge. Furthermore, real-world applications typically require fast algorithms that can run in real time.

## 1.2 Shape-Based Image Segmentation

The task to partition an image into meaningful regions has received considerable attention in the past. When the limits of low-level methods [25], [34], [3] became apparent, researchers endeavored to integrate prior knowledge into segmentation processes. The amount of prior knowledge varies from a part-based (deformable) object structure [15], [14], [35] over a collection of shapes [19], [4], [29], [43], [9], [37], [7], [8], [28] to a single shape [13].

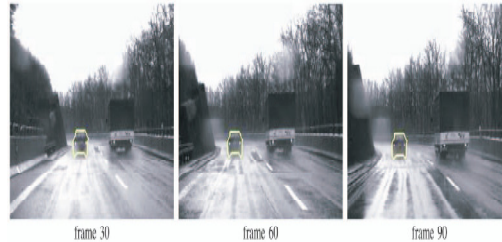


Figure 1. Tracking a car in bad weather: Despite bad visibility, reflections, and camera shake, the proposed method allows reliable tracking over a hundreds of frames

Such methods are bound to find local optima of the energy they are optimizing and heavily depend on the initial contour. In addition, they are based on rather simple shape similarity measures, which do not attempt to establish correspondences of parts or points.

Recently, Cremers et al. [8] dealt with the first point: Starting from an implicit representation of shapes and segmentations, they are able to find globally optimal segmentations while taking into account shape similarity to a number of training shapes. However, the lack of point correspondences remains. In contrast, a number of discrete approaches do allow shape priors based on point correspondences while guaranteeing global optimality: Coughlan et al. [5] are able to match open contours to images, taking into account an elastic shape similarity measure [31], [32]. Being based on dynamic programming, the method is, in principle, parallelizable. However, it is limited to open contours, and hence, does not provide a segmentation. Although the method could be extended to closed contours by performing a complete search over the start point; in practice, this would be far too time-consuming.

The first globally optimal shape-based segmentation algorithm was proposed by Felzenszwalb [13]. It is based on dynamic programming in chordal graphs. The algorithm is easy to parallelize and invariant with respect to translation, rotation, and scale changes. In practice, however, due to its quadratic memory complexity, pixel accurate segmentations can only be computed on rather coarse resolution.

## 1.2 Contribution

In this paper, we present an effectively linear-time algorithm to match contours to images closed contours reduce the bias toward short curves by reverting to ratio functional and minimum ratio cycle computation. The proposed method supports different amounts of invariances, including

translational and rotational ones. By exploiting its high parallelizability, real-time tracking becomes feasible.

### Optimization of GDT'S

Estimating the maximum a posteriori (MAP) solution directly is usually impossible due to the size of the configuration space, even for template models with very few vertices. Instead we have implemented two different optimization techniques for the segmentation and tracking process: Simulated Annealing(SA) minimization technique is used during the segmentation process and Iterated Conditional Modes(ICM) as an efficient local minimization technique is used during the tracking process. Simulated Annealing is a stochastic relaxation technique which generates randomly new configurations by sampling. Iterated Conditional Mode is a deterministic relaxation algorithm. It is very well suited for tracking objects if the temporal resolution is high enough.

## 2 MATCHING'S AS CYCLES IN A PRODUCT SPACE

We are given a prior contour  $S : S^1 \rightarrow \mathbb{R}^2$  (where  $S^1$  is the unit circle) with a uniform parameterization. The task is to match this contour to a given image  $I : \Omega \rightarrow \mathbb{R}^2$ , where  $\Omega \subset \mathbb{R}^2$  is the (typically rectangular) image domain. The placed contour  $C : S^1 \rightarrow \Omega$  should be similar to the input contour and fulfill some data-driven criteria. In this work, we want it to be located at image edges. Figure 2 gives an illustration of our approach: When a contour and an image are input, the algorithm locates a deformed version of the contour in the image and computes an alignment to the prior contour.

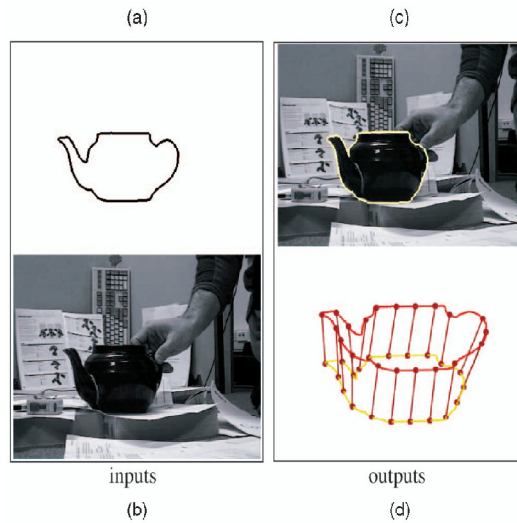


Figure 2 Starting from (a) a prior contour and (b) an input image, the proposed method simultaneously locates (c) the (possibly deformed) contour in the image and computes (d) a correspondence function between the two curves

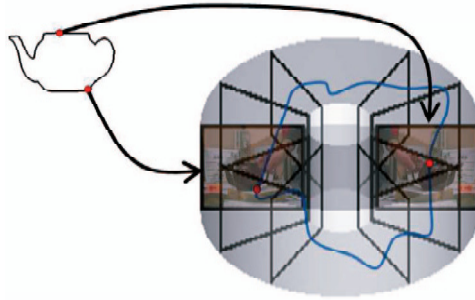


Figure 3 Cyclic paths in a 3D graph (no edges are shown): For any point on the prior contour, there are  $K$  copies of the image in the graph. Any assignment of pixels in the image to corresponding points on the template contour corresponds to a cyclic path in this graph. This allows to use correspondence-based shape similarity measures, which were shown to be important for reproducing human notions of shape similarity [18], [26].

While this was known for open curves [5], the computationally much more challenging case of closed curves has so far not been solved. The product space arises by combining the functions  $C$  and  $m$  into a single function  $\Gamma: S^1 \rightarrow \Omega \times S^1$  which is called a cycle. The space in which these cycles live is visualized in Figure. 3. It has the form of a torus and arises by placing a copy of the image for each point on the (onedimensional) prior contour. When splitting a closed contour at some point, it can be viewed as an open one. The space would then be a solid block. When additionally imposing that start and end points are identical, the respective end faces of the block have to meet and the torus is formed. A curve (with winding number 1) in this space now allows to read off the desired information: The curve  $C$  is obtained by projecting  $\Gamma$  to the first two dimensions. The correspondences of the points on  $C$  can be read off in the third dimension.

### 3 ASSIGNING A COST TO EACH CYCLE

We now present an exemplary energy functional for matching shapes to images. The presented method applies to a much larger class of functionals. For example, in [40], we used a more sophisticated data term based on patch comparison. Before we state the cost function, we briefly discuss how curves are represented.

#### 3.1 Representing Curves

There are infinitely many ways to parameterize a specific curve. Naturally, an optimization problem should not depend on the chosen parameterization.

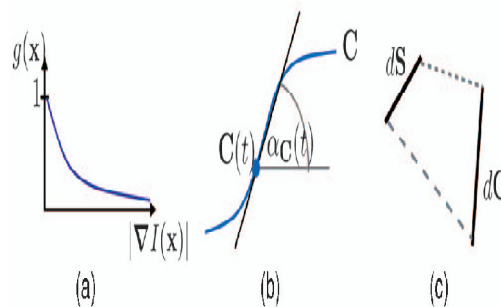


Figure 4 The three ingredients of the proposed method: (a) An edge detector function assigning low values to high image gradients. (b) Computation of tangent angles of the contours  $C$  and  $S$  (shown for  $C$ , the tangent is drawn in black). (c) Computation of length distortion.

The functional we consider in this paper is indeed invariant with respect to reparameterizations. For most of this section, we will therefore not assume any specific parameterization of the contour  $C$  to be optimized. Yet, in a few places, it will be convenient to have a uniform parameterization, i.e., with constant derivative  $\|C_s(s)\| = \|C\|^{-1} kCk$  everywhere. In the given setting, the correspondence function  $m$  is dependent on the contour  $C$ :  $m(s)$  will always denote the correspondence of the point  $C(s)$ . Hence, if the parameterization of  $C$  is changed, the function  $m$  changes as well. In subsequent sections, we prefer the combined function  $\Gamma: S^1 \rightarrow \Omega \times S^1$ . Since the objective function is not invariant against reparameterizations of  $\Gamma$  (data term and shape measure are not coupled), we state it in terms of  $C$  and  $m$ .

We allow self-intersecting contours  $C$  since we have no means to exclude them. We found them to arise only seldom as long as the desired object is truly contained in the image.

#### 4 DISCRETIZING COST AND PRODUCT SPACE

To optimize over the cycles  $\Gamma: S^1 \rightarrow \Omega \times S^1$ , both the cost function and the product space are discretized. This section deals with the discretization, the optimization algorithm is detailed in the next one. The key idea is to represent  $C$  as a polygonal curve with (an a priori unknown number of) vertices on the pixel grid. In addition, the correspondence  $m$  is assumed to be linear along each polygonal line segment. It is therefore uniquely defined by assigning point correspondences to the two end points of such a segment. Specifically, we consider line segments connecting neighboring pixels on the pixel grid, where we choose an 8-neighborhood. A cycle  $\Gamma$  can now be composed out of a finite set of basic parts  $\Delta\Gamma = (\Delta C, \Delta m)$ . 4.1 Discretizing Prior Contour and Correspondence In addition to the cycle  $\Gamma$ , the prior contour  $S$  is also discretized. we represent it in the same form as the contour  $C$ , i.e., as an ordered set  $s_0, \dots, s_{|S|}$  of points on a suitable pixel grid, where—for ease of notation— $s_0 = s_{|S|}$  is represented twice. To get a dense representation of the contour, we require that  $s_i$  be among the eight closest neighbors of  $s_{i-1}$ . The discrete correspondence function assigns each image pixel on  $C$  one of these  $|S| + 1$  prior points. To ensure a monotone matching, we enforce that the start pixel of a segment  $\Delta C$  is assigned a shape point with index lower than or equal to that of the endpoint. Closure of the matching is obtained by the fact that  $s_{|S|} = s_0$ . The length distortion penalizer gives two hard constraints, which limit the minimal and maximal distortion ratio. In the discrete setting, these are realized in terms of the indices of the two shape points assigned to a line segment. The upper limit corresponds to an index difference of at most  $K$ . Ensuring the lower limit is more intricate since here several line segments  $\Delta C$  may correspond to the same part  $s_{i-1} s_i$  of  $S$ . We therefore allow the two indices to be equal.

However, for any shape point  $s_i$ , there may be at most  $K$  parts, where both endpoints of  $\Delta C$  correspond to  $s_i$ . In practice, this is realized by modifying the correspondence function  $m$ : In the discrete setting,  $m$  maps to pairs  $(i, k)$  where  $i$  gives the shape point and  $k < K$  gives the number of image pixels already corresponding to  $s_i$ . If  $m$  maps to the same  $i$  at the beginning and end of the contour segment, then the index  $k$  must be one higher for the end node. This is formalized in the following section.

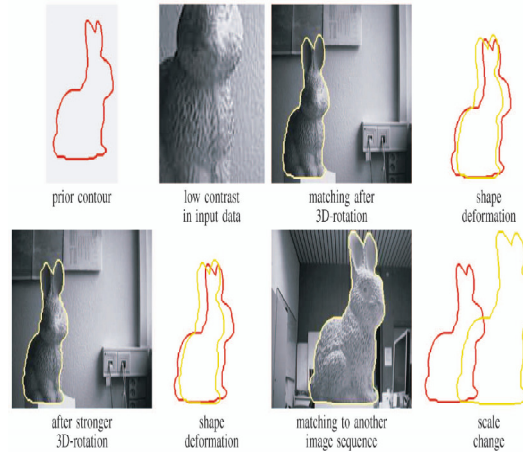


Figure 5 Segmentation with a single template: Despite significant deformation, scale change, and translation, the initial template curve (red) is accurately matched to each template.

## 5 SHAPE - BASED IMAGE SEGMENTATION

We treat images with significant distortion. As a consequence, we allow  $K=5$  image pixels to be matched to a single shape point and set a low length distortion weight with  $\lambda=0.1$ . The tangent angles are given more weight with  $v=0.5$ —this term really drives the process.

### 5.1 Translation-Invariant Matching

In Figure 5, the contour of a rabbit (viewed from the side) is matched to images from two different sequences. In the first sequence, the rabbit is shown from different viewpoints but at the same scale. Despite low contrast between object and background, the algorithm relocates the object reliably.

### 5.2 On the Effect of Length Normalization

We introduced the length normalization to reduce the bias toward shorter curves. This effect is demonstrated in Figure. 6: The figure shows the global optima for the ratio functional and for the numerator integral alone. The latter corresponds to the geodesic energy we proposed in [41]:

$$E_{geo}(\Gamma) = \|\mathbf{C}\| \cdot E(\Gamma)$$

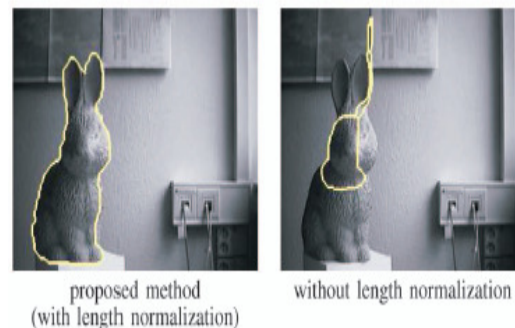


Figure 6 The length normalization removes the bias toward shorter curves.

and is minimized globally by a combination of branch and bound and the shortest path algorithms. Clearly, the ratio functional produces longer curves. We observe this whenever there is low contrast in some regions along the desired curve.

### **5.3 Including Rotational Invariance**

Aside from translational invariance, sometimes one also wants rotational invariance. The proposed framework can be easily extended to include this: One simply samples the rotation angle in sufficiently dense intervals. The prior contour is rotated by the specified amount and the obtained contour is matched to the image.

## **6 SHAPE-BASED TRACKING**

In this section, we present the problem of tracking deformable objects (or contours). In the first frame, the contour  $S$  is given. Then subsequently, we map the contour determined for the previous frame to the current frame. This performs better than keeping a fixed template since large-scale deformations are decomposed into a sequence of smaller ones.

## **7 CONCLUSION**

In this paper, we introduced a polynomial-time solution for matching a given contour to an image despite translation, rotation, scale change, and deformation. The central idea is to cast the assignment of an image pixel to each template point as a problem of finding optimal ratio cycles in a 3D graph that represents the product space of image and template. The energy that is optimized globally consists of an edge-based data term and a shape similarity measure favoring similarity of local edge angles and minimal distortion (stretching/shrinking) of the template curve.

We propose to use an energy-minimizing geometrically deformable template(GDT) which can deform into similar shapes under the influence of image forces. This allows the simultaneous segmentation of multiple deformable objects using intra-as well as inter-shape information. Simulated Annealing(SA).

## **REFERENCES**

- [1] R.E. Bellman, "On a Routing Problem," Quarterly Applied Math., vol. 16, pp. 87-90, 1958.
- [2] A. Blake and M. Isard, Active Contours. Springer Verlag, 1998.
- [3] V. Caselles, R. Kimmel, G. Sapiro, and C. Sbert, "Minimal Surfaces Based Object Segmentation," IEEE Trans. Pattern Analysis and Machine Intelligence, vol. 19, no. 4, pp. 394-398, Apr. 1997.
- [4] T. Cootes and C.J. Taylor, "Active Shape Model Search Using Local Grey-Level Models: A Quantitative Evaluation," Proc. British Machine Vision Conf., pp. 639-648, 1993.
- [5] J. Coughlan, A. Yuille, C. English, and D. Snow, "Efficient Deformable Template Detection and Localization without User Initialization," Computer Vision and Image Understanding, vol. 78, no. 3, pp. 303-319, 2000.
- [6] D. Cremers, "Dynamical Statistical Shape Priors for Level Set Based Tracking," IEEE Trans. Pattern Analysis and Machine Intelligence, vol. 28, no. 8, pp. 1262-1273, Aug. 2006.



- [7] D. Cremers, S.J. Osher, and S. Soatto, "Kernel Density Estimation and Intrinsic Alignment for Shape Priors in Level Set Segmentation," *Int'l J. Computer Vision*, vol. 69, no. 3, pp. 335-351, Sept. 2006.
- [8] D. Cremers, F.R. Schmidt, and F. Barthel, "Shape Priors in Variational Image Segmentation: Convexity, Lipschitz Continuity and Globally Optimal Solutions," *Proc. IEEE Int'l Conf. Computer Vision and Pattern Recognition*, June 2008.
- [9] D. Cremers, F. Tischhauser, J. Weickert, and C. Schnorr, "Diffusion Snakes: Introducing Statistical Shape Knowledge into the Mumford-Shah Functional," *Int'l J. Computer Vision*, vol. 50, no. 3, pp. 295-313, 2002.
- [10] F. Dellaert and C. Thorpe, "Robust Car Tracking Using Kalman Filtering and Bayesian Templates," *Proc. Conf. Intelligent Transportation Systems*, 1997.
- [11] J. Denzler and H. Niemann, "Active Rays: Polar-Transformed Active Contours for Real-Time Contour Tracking," *Real-Time Imaging*, vol. 5, pp. 203-213, 1999.
- [12] A. Doucet, N. de Freitas, and N. Gordon, *Sequential Monte Carlo Methods in Practice (Statistics for Engineering and Information Science)*. Springer Verlag, 2001.
- [13] P.F. Felzenszwalb, "Representation and Detection of Deformable Shapes," *IEEE Trans. Pattern Analysis and Machine Intelligence*, vol. 27, no. 2, pp. 208-220, Feb. 2005.
- [14] P.F. Felzenszwalb and D. Huttenlocher, "Pictorial Structures for Object Recognition," *Int'l J. Computer Vision*, vol. 61, no. 1, pp. 55-79, 2005.
- [15] M.A. Fischler and R.A. Eschlager, "The Representation and Matching of Pictorial Structures," *IEEE Trans. Computers*, vol. 22, no. 1, pp. 67-92, Jan. 1973.
- [16] L.R. Ford, "Network Flow Theory," Paper P-923, The Rand Corporation, 1956.
- [17] W. Förstner and E. Gülich, "A Fast Operator for Detection and Precise Localization of Distinct Points, Corners and Circular Features," *Proc. Intercommission Conf. Fast Processing of Photogrammetric Data*, pp. 281-305, 1987.
- [18] Y. Gdalyahu and D. Weinshall, "Flexible Syntactic Matching of Curves and Its Application to Automatic Hierarchical Classification of Silhouettes," *IEEE Trans. Pattern Analysis and Machine Intelligence*, vol. 21, no. 12, pp. 1312-1328, Dec. 1999.
- [19] U. Grenander, Y. Chow, and D.M. Keenan, *Hands: A Pattern Theoretic Study of Biological Shapes*. Springer Verlag, 1991.
- [20] L. Gui, J. Thiran, and N. Paragios, "Joint Object Segmentation and Behaviour Classification in Image Sequences," *Proc. IEEE Int'l Conf. Computer Vision and Pattern Recognition*, 2007.
- [21] G.D. Hager and P.N. Belhumeur, "Real-Time Tracking of Image Regions with Changes in Geometry and Illumination," *Proc. IEEE Int'l Conf. Computer Vision and Pattern Recognition*, pp. 403-410, 1996.
- [22] C. Harris and M. Stephens, "A Combined Corner and Edge Detector," *Proc. Fourth Alvey Vision Conf.*, pp. 147-151, 1988.
- [23] A. Jalba, M. Wilkinson, and J. Roerdink, "CPM: A Deformable Model for Shape Recovery and Segmentation Based on Charged Particles," *IEEE Trans. Pattern Analysis and Machine Intelligence*, vol. 26, no. 10, pp. 1320-1335, Oct. 2004.
- [24] I.H. Jermyn and H. Ishikawa, "Globally Optimal Regions and Boundaries as Minimum Ratio Weight Cycles," *IEEE Trans. Pattern Analysis and Machine Intelligence*, vol. 23, no. 10, pp. 1075-1088, Oct. 2001.
- [25] M. Kass, A. Witkin, and D. Terzopoulos, "Snakes: Active Contour Models," *Int'l J. Computer Vision*, vol. 1, no. 4, pp. 321-331, 1988.
- [26] L.J. Latecki and R. Lakämper, "Shape Similarity Measure Based on Correspondence of Visual Parts," *IEEE Trans. Pattern Analysis and Machine Intelligence*, vol. 22, no. 10, pp. 1185-1190, Oct. 2000.
- [27] E.L. Lawler, "Optimal Cycles in Doubly Weighted Linear Graphs," *Proc. Int'l Symp. Theory of Graphs*, pp. 209-213, 1966.

- [28] V. Lempitsky, A. Blake, and C. Rother, "Image Segmentation by Branch-and-Mincut," Proc. European Conf. Computer Vision, Oct. 2008.
- [29] M. Leventon, W. Grimson, and O. Faugeras, "Statistical Shape Influence in Geodesic Active Contours," Proc. IEEE Int'l Conf. Computer Vision and Pattern Recognition, vol. 1, pp. 316-323, 2000.
- [30] D. Lowe, "Object Recognition from Local Scale-Invariant Features," Proc. IEEE Int'l Conf. Computer Vision, Sept. 1999.
- [31] M. Maes, "Polygonal Shape Recognition Using String-Matching Techniques," Pattern Recognition, vol. 24, no. 5, pp. 433-440, 1991.
- [32] R. McConnell, R. Kwok, J.C. Curlander, W. Kober, and S.S. Pang, "Correlation and Dynamic Time Warping: Two Methods for Tracking Ice Floes in SAR Images," IEEE Trans. Geosciences and Remote Sensing, vol. 29, no. 11, pp. 1004-1012, Nov. 1991.
- [33] E.F. Moore, "The Shortest Path through a Maze," Proc. Int'l Symp. Theory of Switching, pp. 285-292, 1959.
- [34] D. Mumford and J. Shah, "Optimal Approximations by Piecewise Smooth Functions and Associated Variational Problems," Comm. Pure and Applied Math., vol. 42, pp. 577-685, 1989.
- [35] D. Ramanan and C. Sminchisescu, "Training Deformable Models for Localization," Proc. IEEE Int'l Conf. Computer Vision and Pattern Recognition, pp. 206-213, June 2006.
- [36] M. Rousson and D. Cremers, "Efficient Kernel Density Estimation of Shape and Intensity Priors for Level Set Segmentation," Proc. Int'l Conf. Medical Image Computing and Computer Assisted Intervention, vol. 1, pp. 757-764, 2005.
- [37] M. Rousson and N. Paragios, "Shape Priors for Level Set Representations," Proc. European Conf. Computer Vision, pp. 78- 92, 2002.
- [38] T. Schoenemann and D. Cremers, "Globally Optimal Image Segmentation with an Elastic Shape Prior," Proc. IEEE Int'l Conf. Computer Vision, Oct. 2007.
- [39] T. Schoenemann and D. Cremers, "Globally Optimal Shape-Based Tracking in Real-Time," Proc. IEEE Int'l Conf. Computer Vision and Pattern Recognition, June 2008.
- [40] T. Schoenemann and D. Cremers, "Matching Non-Rigidly Deformable Shapes across Images: A Globally Optimal Solution," Proc. IEEE Int'l Conf. Computer Vision and Pattern Recognition, June 2008.
- [41] T. Schoenemann, F.R. Schmidt, and D. Cremers, "Image Segmentation with Elastic Shape Priors via Global Geodesics in Product Spaces," Proc. British Machine Vision Conf., Sept. 2008.
- [42] J. Shi and C. Tomasi, "Good Features to Track," Proc. IEEE Int'l Conf. Computer Vision and Pattern Recognition, June 1994.
- [43] A. Tsai, A. Yezzi, W. Wells, C. Tempny, D. Tucker, A. Fan, E. Grimson, and A. Willsky, "Model-Based Curve Evolution Technique for Image Segmentation," Proc. IEEE Int'l Conf. Computer Vision and Pattern Recognition, pp. 463-468, 2001.
- [44] X. Xie and M. Mirmehdi, "MAC: Magnetostatic Active Contour Model," IEEE Trans. Pattern Analysis and Machine Intelligence, vol. 30, no. 4, pp. 632-646, Apr. 2008.
- [45] C. Xu and J. Prince, "Generalized Gradient Vector Flow External Forces for Active Contours," Signal Processing, vol. 71, no. 2, pp. 131-139, 1998.